Electronic Supplementary Material (ESI) for Journal of Materials Chemistry C.

Supplementary Information

High Performance Solution Processed Oxide Thin-Film Transistors with Inkjet Printed Ag Source-Drain Electrodes

Liam Gillan, Jaakko Leppäniemi, Kim Eiroma, Himadri Majumdar, and Ari Alastalo.

VTT Technical Research Centre of Finland Ltd
E-mail: liam.gillan@vtt.fi
Address: Tietotie 3, Espoo, FI-02044, Finland

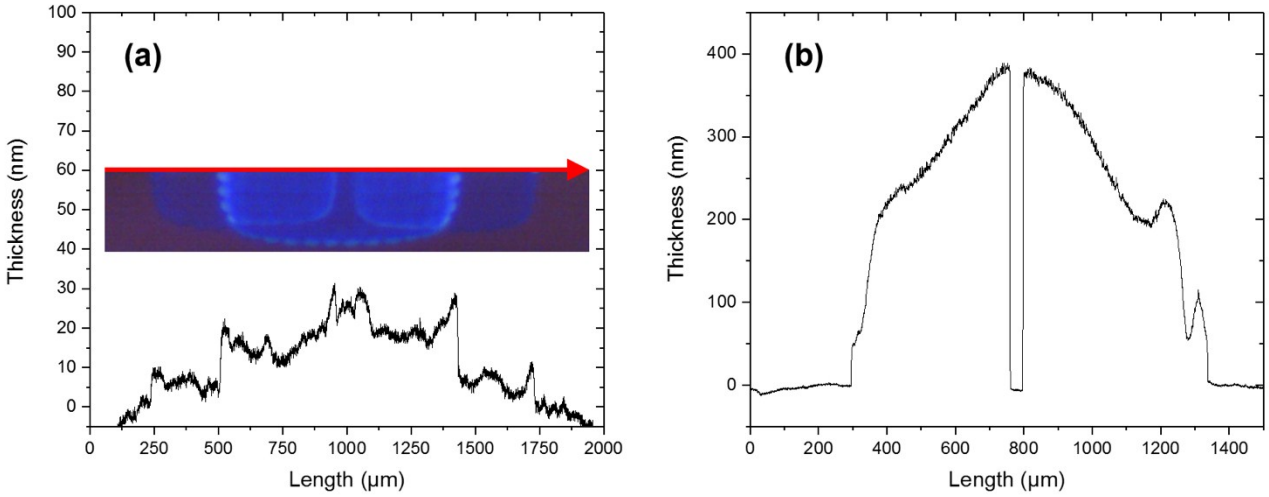

Fig. S1. Stylus profilometer scans of (a) 0.1 wt% PEI–In_2O_3 over In_2O_3, with red arrow indicating scan direction, and (b) Ag S/D contact electrode, with a central scratch through Ag to the Si substrate.

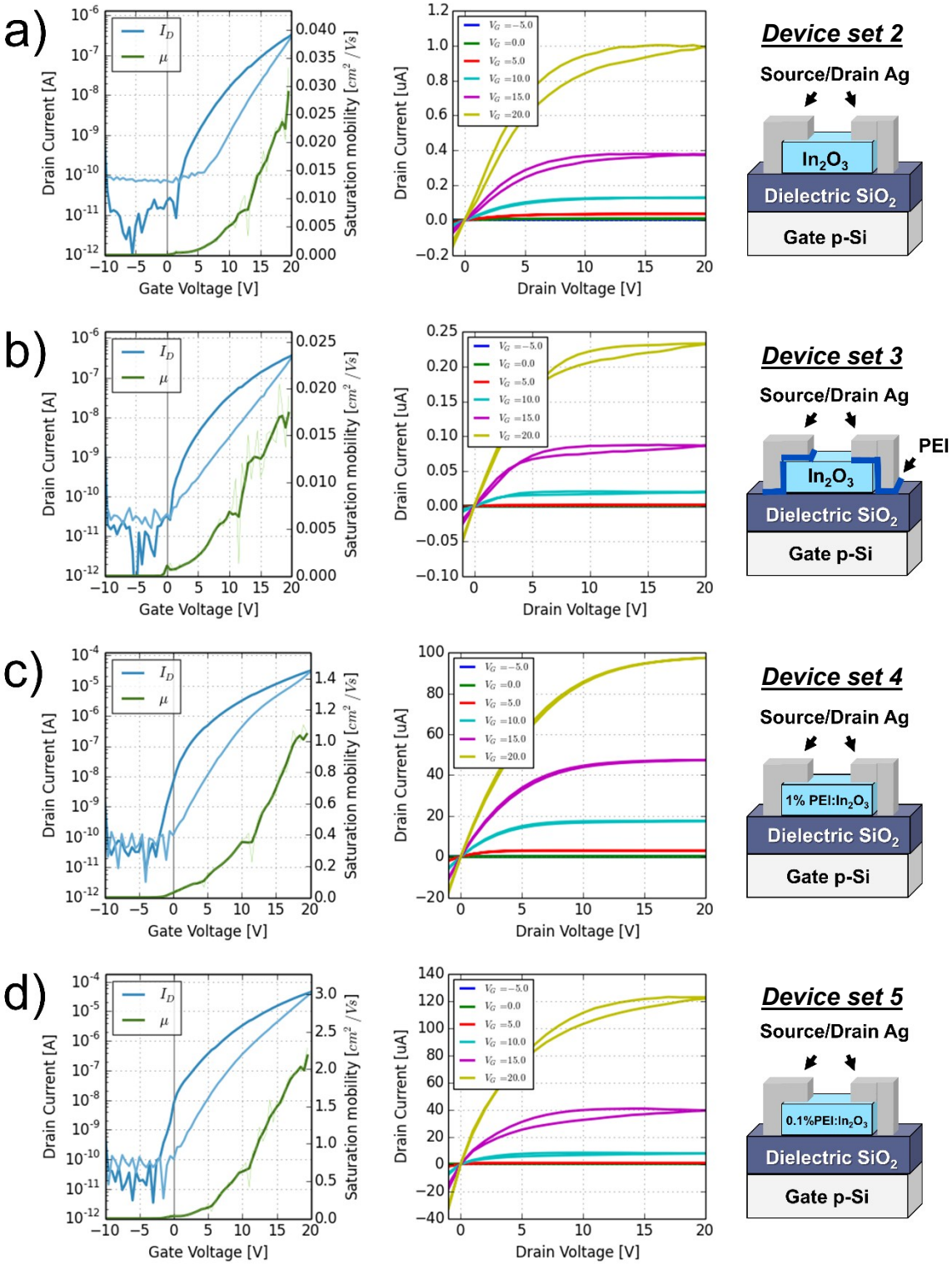

Fig. S2(i). Transfer and output curves of TFT device sets from Table 1 of the manuscript, with varying architecture and material composition (a-d).

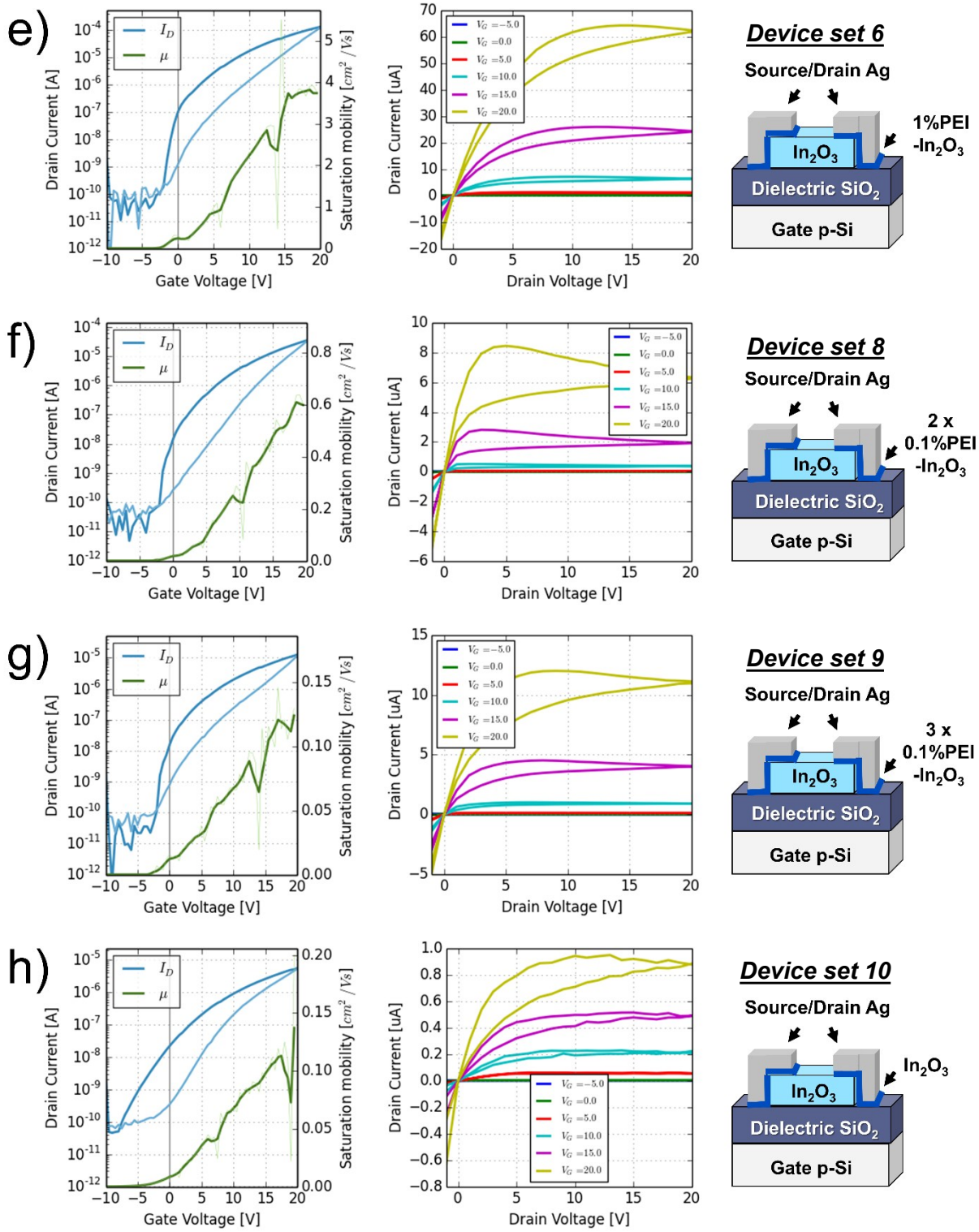

Fig. S2(ii). Transfer and output curves of TFT device sets from Table 1 of the manuscript, with varying architecture and material composition (e-h).

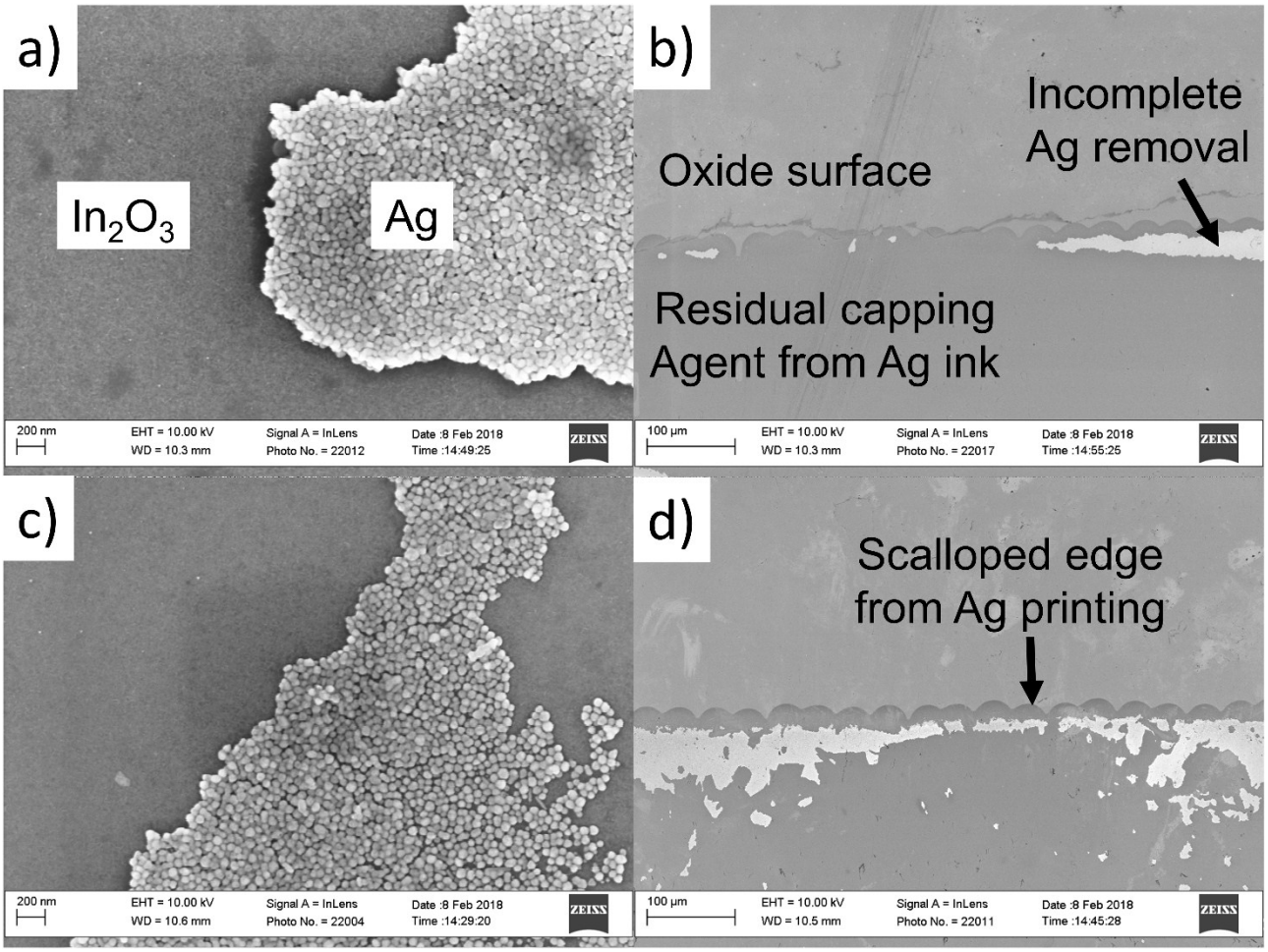

Fig.S3. Scanning electron microscope images of spin coated In_2O_3 (a and b) and 0.1 wt % PEI–In_2O_3 (c and d) following solvent assisted delamination of printed Ag. Dark areas remain after Ag removal (b and d), suspected to be residual capping agent from the Ag nanoparticles. Following Ag removal, some regions of Ag remained as discrete particulates sintered together (a and c).

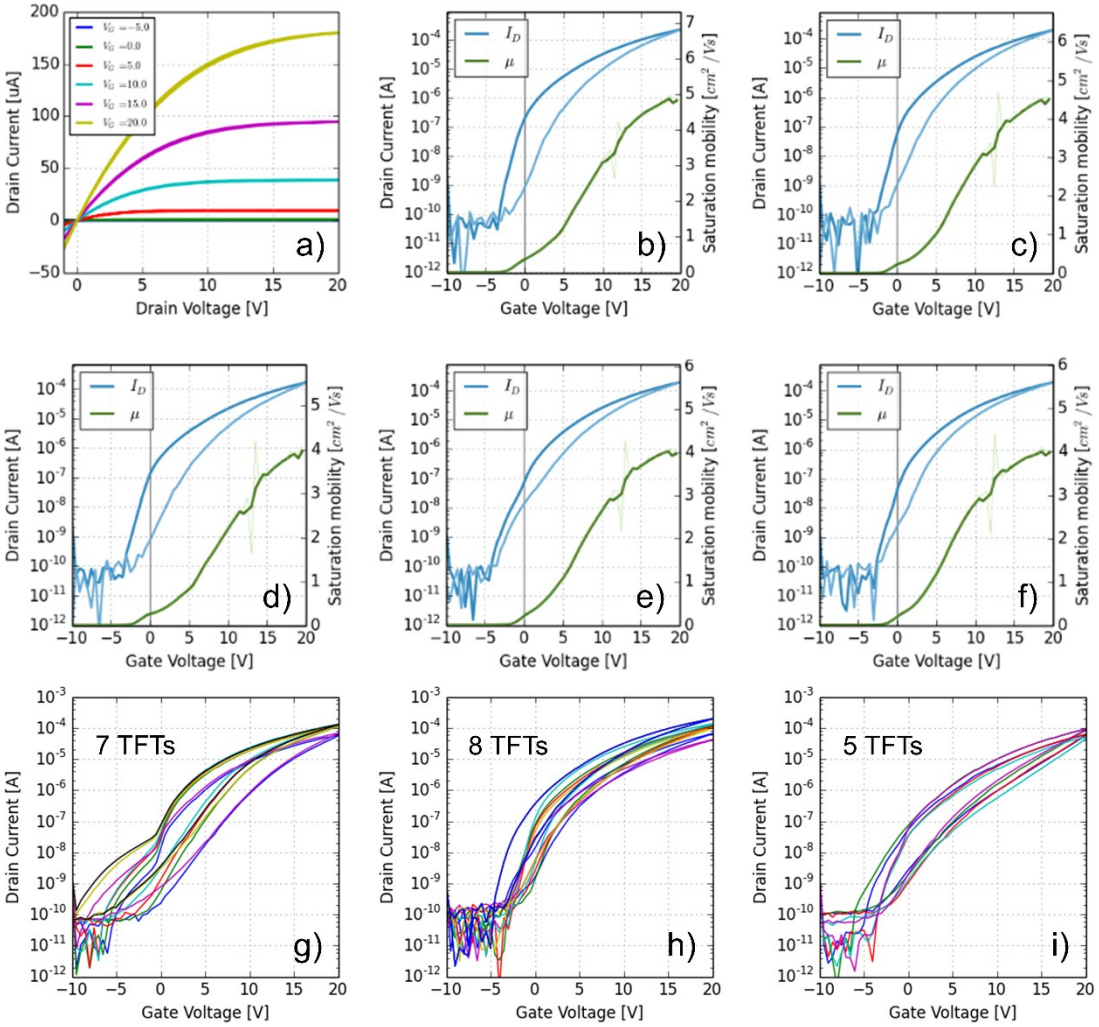

Fig. S4. Output a) and transfer b-f) curves of TFTs from the same sample as Fig. 1b, having In_2O_3 semiconductor, 0.1 wt% PEI–In_2O_3 interlayer, and Ag source/drain contacts (Table 1, Device set 7). To illustrate uniformity across multiple samples, g), h, and i) depict transfer curves of TFTs from three different samples with In_2O_3 semiconductor, 0.1 wt% PEI–In_2O_3 interlayer, and Ag source/drain contacts. The data from these samples was combined with data from the sample presented in Fig. S4b-f, to generate electrical characteristics listed in Table 1, Device set 7.

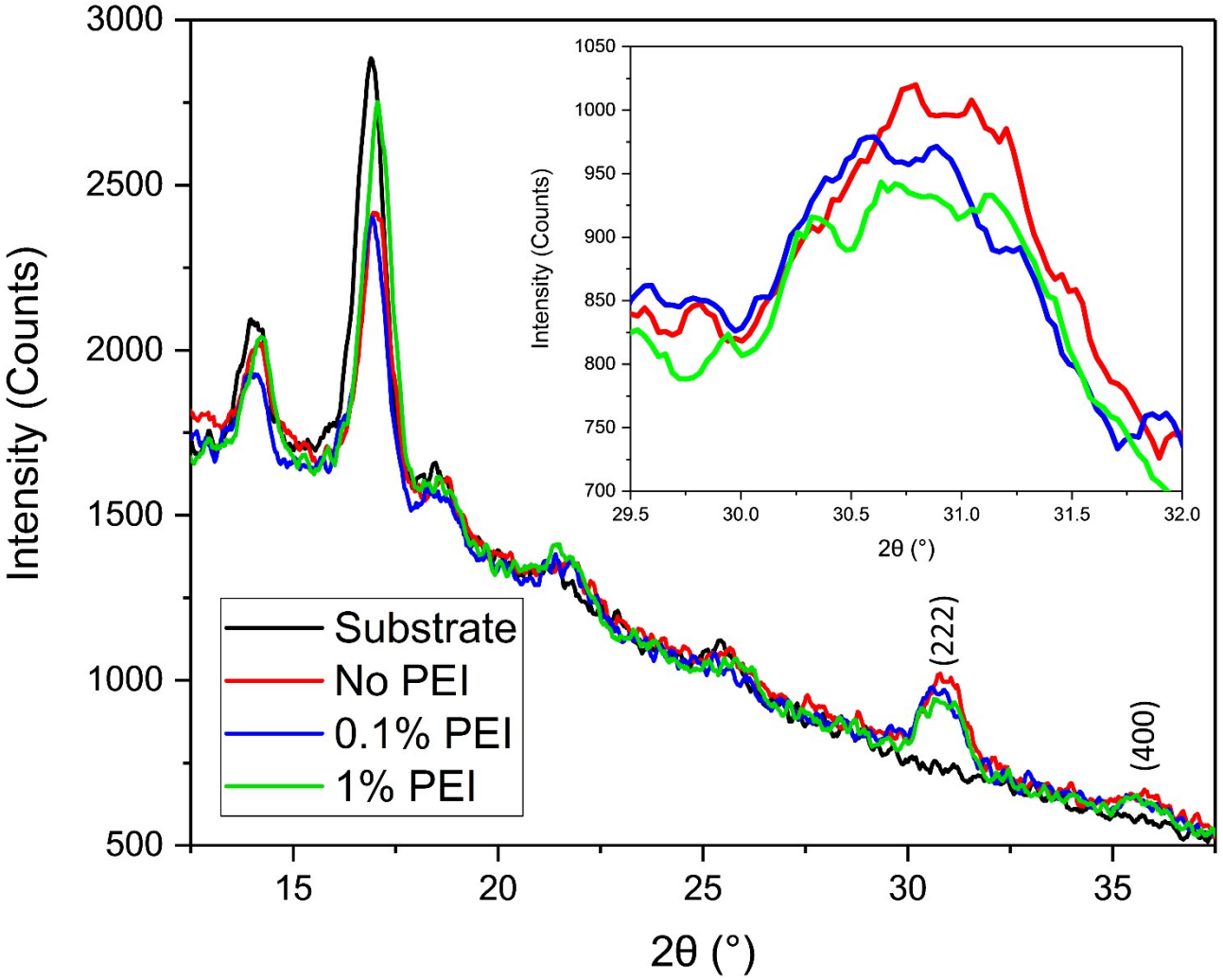

Fig. S5. Grazing incidence X-ray diffraction patterns of intrinsic and PEI doped In_2O_3 films spin coated on Si/SiO_2 substrates, showing that the In_2O_3 (222) crystal peak at 2 theta ∽31° remains upon PEI doping. Data subjected to x-axis ten point smoothing.

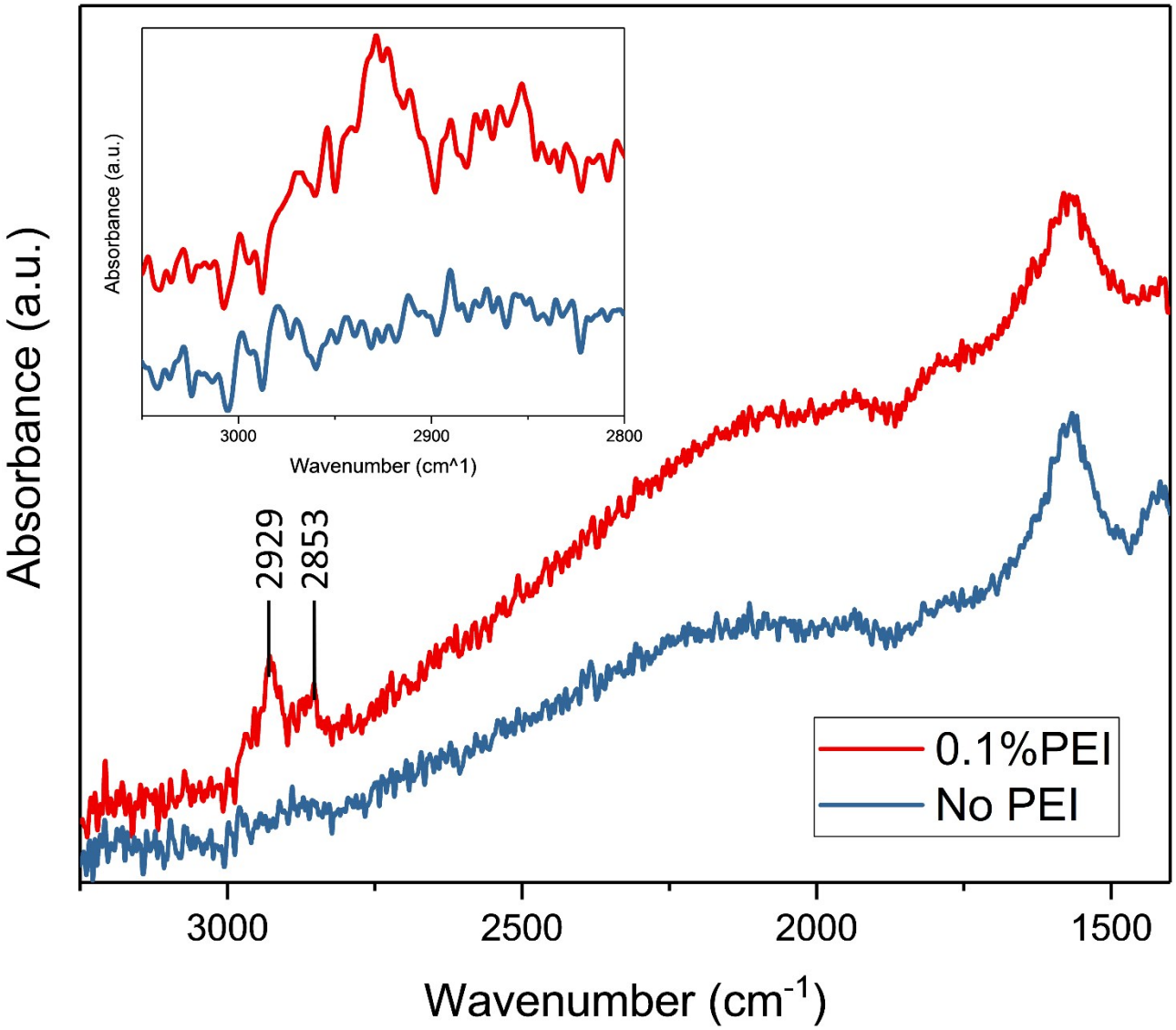

Fig. S6. Fourier transform infrared spectra of spin coated intrinsic and PEI doped In_2O_3 showing increased C-H signal peaks at 2929 and 2853 cm^{-1} as a result of the PEI carbon skeleton.

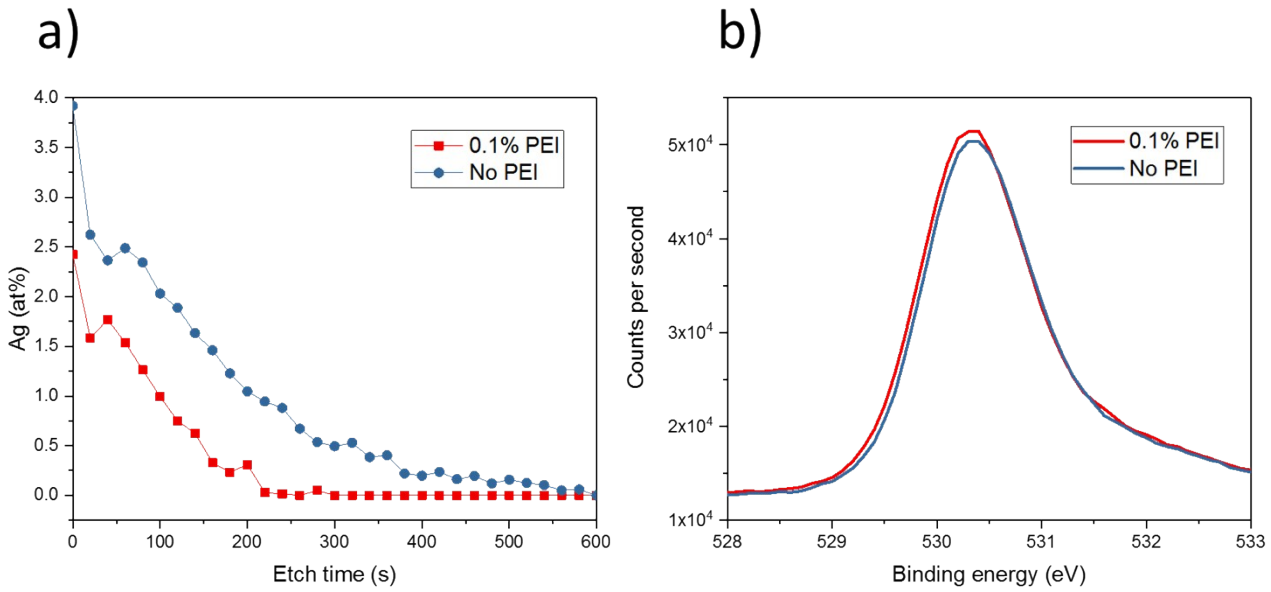

Fig. S7. a) Depth profile X-ray photoelectron spectra of spin coated In_2O_3 and 0.1 wt% PEI–In_2O_3 films on Si/SiO_2 substrate, a) after solvent assisted delamination of printed Ag, showing atomic % concentration of Ag relative to O, In, and Si. Samples were etched to the substrate (∽400 s) by sputtering with 5 eV Ar-ions with 2 mA current and 1x1mm^2 area. Analysis area of 110 µm diameter Ag 3d signal was normalised to that of In 3p in both samples to enable inter-sample comparison. b) O 1s spectra after 60 s sputtering below the film surfaces, presenting striking similarity between intrinsic and PEI doped In_2O_3.

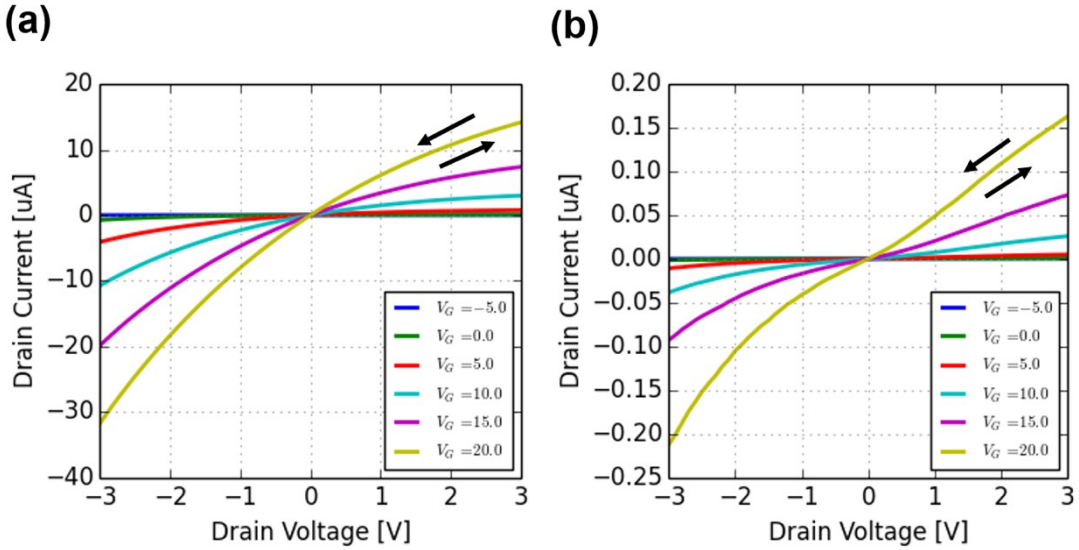

Fig. S8. Output curves for TFTs with (a) inkjet-printed Ag on 0.1 wt% PEI–In_2O_3, showing more ohmic like contact (linear relation), and (b) inkjet printed Ag on In_2O_3, showing more Schottky like contact (upwards curvature).

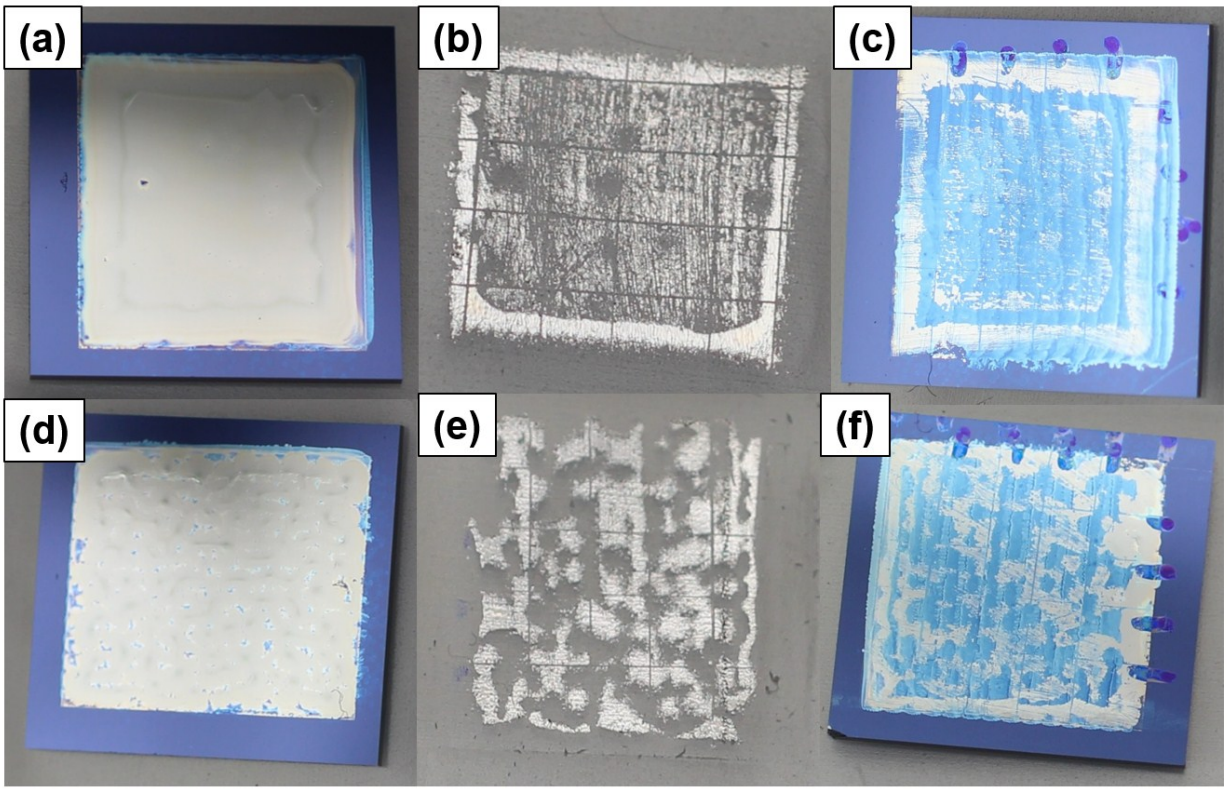

Fig. S9. Adhesion testing of (a) inkjet-printed Ag on In_2O_3, with (b) showing Ag removed by tape, resulting in (c). Stronger adhesion was noted for (d) inkjet-printed Ag on 0.1 wt% PEI–In_2O_3, as indicated by (e) having less Ag removed by tape, resulting in (f) a greater amount of Ag remaining on the sample.